Aceh Int. J. Sci. Technol., 6(3): 104-110
December 2017
doi: 10.13170/aijst.6.3.8116

Aceh International Journal of Science and Technology
ISSN: p-2088-9860; e-2503-2398
Journal homepage: http://jurnal.unsyiah.ac.id/aijst

Residual Radioisotopes Generated from Neutron Irradiated Aluminum Capsules

Imam Kambali[1]*, Indra Saptiama[1,2], Hari Suryanto[1]
[1]Center for Radioisotope and Radiopharmaceutical Technology, National Nuclear Energy Agency (BATAN), Puspiptek Area, Serpong, South Tangerang, Indonesia
[2]Proton Medical Research Center, Tsukuba University, Japan
*Corresponding email: imamkey@batan.go.id

Received : Juli 29, 2017
Accepted: September, 9, 2017
Online : December 31, 2017

Abstract – Aluminum (Al) is often used to house a molybdenum oxide (MoO_3) target for neutron or proton-produced technetium-99m (^{99m}Tc) radioisotope. During neutron or proton bombardment of an Al body, residual radioisotopes could be generated following nuclear reactions between the incoming particles and the Al body. In this research, residual radioisotopes produced following nuclear reactor based-neutron irradiation of Al body were experimentally measured using a portable gamma ray spectroscopy system; whereas TALYS 2015 calculated data were used to evaluate various nuclear reactions for the by-product identification. As a comparison, Al body used in a cyclotron-based ^{99m}Tc production was also analyzed. Experimental data indicated that relatively long-lived radioisotopes such as ^{26}Al, ^{22}Na and ^{24}Na were identified in the Al body following nuclear reactor-based ^{99m}Tc production, whereas the presence of ^{27}Mg radioisotope was, for the first time, experimentally detected in both the Al bodies for nuclear reactor-based and cyclotron-based ^{99m}Tc production. A special safety attention should be paid to the radiation workers when producing ^{99m}Tc using a nuclear reactor since it generates ^{26}Al (half-life = 716,600 years).

Key words: aluminum, neutron, proton, radioisotope, residual.

Introduction

Technetium-99m is a radioisotope commonly used in nuclear medicine for diagnosis of cardiac-related diseases (Lu *et al* 2015; de Haro-del Moral *et al* 2012), liver related cancers (Gates *et al* 2015; Conway *et al* 2013), breast cancers (Pinker *et al* 2011; Silov *et al* 2014) and prostate cancers (Hillier *et al* 2013; Vallabhajosula *et al* 2014). The gamma emitting radioisotope is produced via $^{99}Mo(n,p)^{99}Mo \rightarrow ^{99m}Tc$ nuclear reaction by exposing molybdenum (Mo) target in neutron beams generated in a nuclear reactor (Pillai *et al* 2013). In the target preparation, MoO_3 target is encapsulated in an aluminum body and then it is placed in a target holder prior to neutron irradiation. During the irradiation, nuclear reactions are expected to occur between the neutrons and Mo target as well between the neutrons as Al capsule.

Another relatively new method of producing ^{99m}Tc is using proton beams generated by cyclotrons, in which enriched Mo target (^{100}Mo) is irradiated via $^{100}Mo(p,2n)^{99m}Tc$ nuclear reaction. Similar to the nuclear-reactor based ^{99m}Tc production, the latter method also employs Al body to house the enriched ^{100}Mo target. Therefore, comprehensive theoretical and experimental studies on the residual radioisotopes generated during ^{99m}Tc production are of paramount importance since they correspond to the radiation worker's safety concerns.

Research on residual radionuclides generated during proton bombardment of enriched water target for ^{18}F radionuclide production has been carried out earlier (Kambali *et al* 2016) whereas radioactive by-products have also been detected on a wall of a cyclotron (Kambali & Suryanto 2016). In case of Al target, recent theoretical studies suggested that long-lived ^{26}Al and ^{24}Na could be produced from fast neutrons-irradiated Al target (Saran *et al* 2012). Using neutron activation analysis, Kinomura and coworkers (Kinomura *et al* 2002) also identified ^{24}Na radioisotope which was presumably produced from neutron-induced ^{27}Al when a Ti-Al alloy was irradiated by fast neutrons. Similar investigation is, therefore, required to better understand the origin of residual radioactive sources and also as part of safety measures applied in

the neutron-based ^{99m}Tc routine production at the Gerrit Agustinus Siwabessy (G.A. Siwabessy) nuclear reactor in Indonesia as well as experimental proton-based ^{99m}Tc production using a cyclotron.

In this investigation, possible nuclear reactions and residual radioisotopes produced when cold, thermal and fast neutrons in the energy range of 0 to 50 MeV hit Al capsule are studied from their nuclear cross-sections using the TALYS 2014 codes (Koning & Rochman 2012). Moreover, experimental data on residual radioisotopes generated from cyclotron-produced ^{99m} Tc are compared with that of nuclear reactor-produced ^{99m}Tc..

Materials and Methods

Direct Neutron Irradiation

A locally made Al body was employed to encapsulate MoO_3 target. The target was placed in the Central Irradiation Position (CIP) of the G.A. Siwabessy nuclear reactor in Serpong, Indonesia, and then directly irradiated with neutrons at a neutron flux of 1.12×10^{14} n.cm^{-2}.s^{-1} for 5 days. The neutron irradiation procedure has been discussed elsewhere (Saptiama *et al* 2016). Once the irradiation was completed, the Al body was separated from the MoO_3 target and cooled for 4 hours to allow short-lived residual radioisotopes to decay so that the radiation exposure would decrease to a relatively safer level. During the measurement, an exposure of 13 mSv was detected on the outer surface of the Al body at a distance of 1 m.

Secondary Neutron Irradiation

In the secondary neutron irradiation, an aluminum body was used as a target holder for cyclotron-based ^{99m}Tc production via ^{100}Mo(p,2n)^{99m}Tc nuclear reaction. An 11-MeV proton beam generated from a cyclotron was directed to a solid natural MoO_3 target consisting of 9.63% atomic weight of Mo-100 during ^{99m}Tc production. During the bombardment, the proton beam was kept at a constant current of 10 μA while the irradiation time was set to be 10 minutes. Secondary neutrons as a result of the ^{100}Mo(p,2n)^{99m}Tc were expected to hit the aluminum holder; thus this routine would result in the production of residual radionuclides. The procedures for proton irradiation using an 11-MeV cyclotron have been previously discussed elsewhere (Kambali *et al* 2016).

Gamma Ray Detection and Identification

A portable gamma ray spectroscopy system consisting of a pocket MCA (Type MCA8000A) made by Amptek, USA with the serial number 2278 coupled to a NaI(Tl) detector was employed to identify the radioactive by-products present in the Al capsules. The energy calibration of the spectroscopy system was performed using ^{137}Cs, ^{60}Co and ^{241}Am standard radioactive sources as discussed elsewhere (Kambali *et al* 2016; Kambali & Suryanto 2016a; Kambali & Suryanto 2016b). The background-subtracted gamma ray spectrum of the Al capsules was then analyzed for samples irradiated using the G.A Siwabessy nuclear reactor and the 11-MeV cyclotron.

Theoretical Calculations

In this study, the TALYS nuclear model (Koning & Rochman 2012) was used to calculate nuclear cross-sections of the (n,γ), (n,α), (n,p), (n,2n), (n,nα), (n,d) and (n,2nα) reactions for a broad range of neutron energies ranging from cold neutrons (0.00001 eV) to fast neutrons (of up to 200 MeV). The TALYS codes have been widely used elsewhere (Kambali 2014; Bakhtiari *et al* 2013).

Results and Discussion

Predicted Nuclear Reactions and Radioisotopes

Nuclear reactions potentially occur when neutrons hit Al target and this can be predicted from their nuclear cross-sections. TALYS-calculated nuclear cross-sections of up to 150-MeV neutrons are shown in Fig. 1 which indicate that (n,α) and (n,p) nuclear reactions dominate at neutron energies between 1 and 20 MeV, whereas (n,2n), (n,nα), (n,d) and (n,2nα) are significant at neutron energies over 20 MeV. In addition, (n,γ) nuclear reactions are of importance at thermal energy (Fig. 1, inset). While the maximum cross-sections for (n,2nα) nuclear reaction is only 13.14 mbarn at neutron energy of 46 MeV, the rest of the nuclear reactions investigated here show nuclear cross-sections of greater than 60 mbarn at neutron energies of lower than 40 MeV.

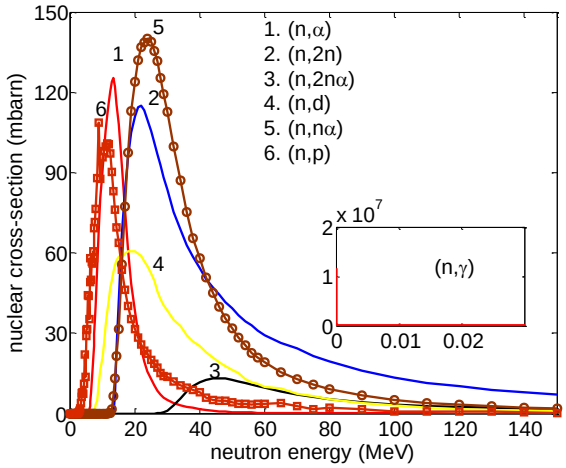

Figure.1 TALYS calculated (n,γ), (n,α), (n,2n), (n,2nα), (n,d), (n,na), and (n,p) nuclear reactions of Al target

Based on the above nuclear cross-sections, there are several radioactive isotopes potentially generated during neutron bombardment of an Al target, including ^{28}Al which could be produced via ^{27}Al(n,γ)^{28}Al reaction, ^{26}Al generated through ^{27}Al(n,2n)^{26}Al reaction, ^{22}Na produced via ^{27}Al(n,2nα)^{22}Na reaction, ^{27}Mg generated through ^{27}Al(n,p)^{27}Mg reaction, ^{24}Na produced via ^{27}Al(n,α)^{24}Na reaction, and ^{30}Si generated through ^{27}Al(n,d)^{30}Si reaction. In addition, stable isotope ^{23}Na could also be generated via ^{27}Al(n,nα)^{23}Na reaction.

Possible Particle Production

During neutron irradiation of Al target, apart from secondary neutron production, some other particles such as protons, deuterons and alphas could also potentially be generated as can be seen from their nuclear cross-sections (Figure 2). Among the four particles, deuteron production is expected to have the lowest nuclear cross-section and production yield, whereas secondary neutron production has the highest nuclear cross-section and production yield. In general, for incoming neutron energies over 30 MeV, both nuclear cross-sections and production yields increase with increasing neutron energies. For neutron energies greater than 100 MeV, both secondary neutron and proton yields are greater than 1, whereas the yields of the other particles (deuterons and alphas) are lower than 1 as seen in Figure 2, inset.

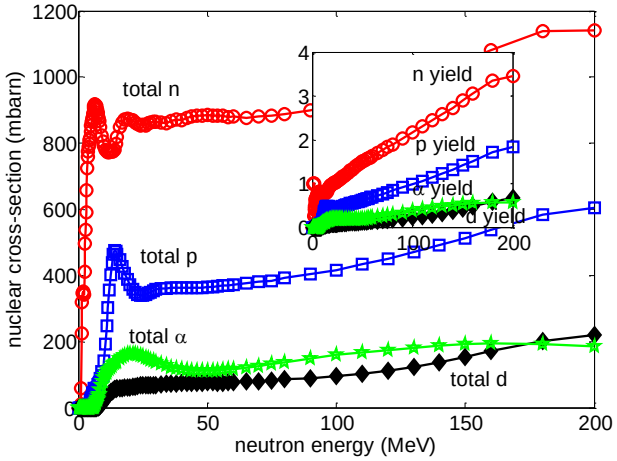

Figure 2 Total cross-sections and production yields of n, p, α and d particles in neutron-irradiated Al target calculated using TALYS codes.

Production of secondary particles could result in generation of either radioactive or stable isotopes when the particles hit materials around them.

1. Secondary alpha particle reactions with Al target

Based on TALYS 2015-calculated nuclear cross-sections, the most significantly possible reactions are (α,p) and (α,n) nuclear reactions which have maximum cross-sections of 287 and 207 mbarn at 11 MeV alpha particles, respectively. The expected isotopes generated when alpha particles hit Al target are stable isotope ^{30}Si as a result of ^{27}Al(α,p)^{30}Si nuclear reaction and radioisotope ^{30}P due to ^{27}Al(α,n)^{30}P reaction. As a positron (β^+) emitter and with a half life of 4.298 minutes, ^{30}P could be experimentally observable with an appropriate gamma ray detecting system.

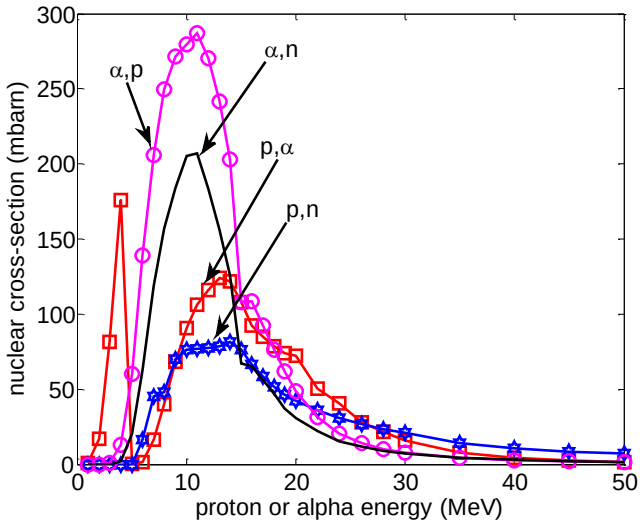

Figure 3 Nuclear cross-sections of secondary α and p particle-induced Al target

2. Secondary proton reactions with Al target

   Calculations using TALYS 2015 codes (Fig. 3) indicate that only (p,n) reaction is significant with a maximum nuclear cross-section of 81.2 mbarn at proton energy of 14 MeV, whereas for (p,2n) the maximum nuclear cross-section is just 1.53 mbarn at 35-MeV protons. In this case, ^{27}Si radionuclide – a β^+ emitter with a half life of 4.160 seconds – could be produced via ^{27}Al(p,n)^{27}Si nuclear reaction, whereas ^{26}Si radionuclide – also a β^+ emitter with a half life of 2.234 seconds – could be generated via ^{27}Al(p,2n)^{26}Si nuclear reaction, though the latter radioactive yield maybe insignificant due to low cross-section and high threshold energy.

3. Secondary deuteron reactions with Al target

   Again, based on TALIS 2015 calculated data (Fig. 4), there are several possible nuclear reactions should secondary deuterons hit Al target, including (d,p), (d,2p), (d,n), (d,2n) and (d,α) reactions. The maximum nuclear cross-sections for the aforementioned reactions vary depending on the incoming deuterons, with the highest cross-section of 285 mbarn for (d,n) reaction at 4 MeV-deuterons. Two stable isotopes and 3 radioactive isotopes could be generated from these reactions, namely ^{28}Si stable isotope created from ^{27}Al(d,n)^{28}Si reaction, ^{25}Mg stable isotope produced via ^{27}Al(d,α)^{25}Mg reaction, ^{28}Al radioisotope generated from ^{27}Al(d,p)^{28}Al reaction, ^{27}Mg radioisotope as a result of ^{27}Al(d,2p)^{27}Mg reaction, and ^{27}Si radioisotope due to ^{27}Al(d,2n)^{27}Si reaction.

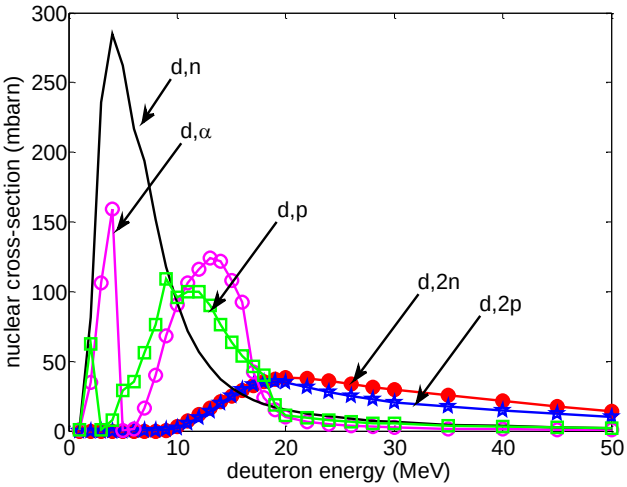

Figure 4 Nuclear cross-sections of secondary d-particle-induced Al target

To summarize, Table 1 presents all expectedly produced isotopes following neutron and proton irradiation of Al target. In addition, other secondary particles such as alpha and deuteron are also responsible for the creation of various radioactive and stable isotopes. The half lives of the radioisotopes vary from as short as 4.142 seconds to 716,600 years, while the emitted particles from the radioactive decays are mostly β^+ particles, though other particles such as γ and β^- could also be part of the decay modes.

Table 1 Predicted secondary particles and their associated isotopes produced from primary neutron and proton interactions with Al target

Secondary particle	Isotope	Half life	Nuclear Reaction	Remarks
neutron	^{26}Al	716,600 years	^{27}Al(n,2n)^{26}Al	β^+ emitter
	^{22}Na	2.605 years	^{27}Al(n,2nα)^{22}Na	β^+ emitter
	^{27}Mg	9.458 minutes	^{27}Al(n,p)^{27}Mg	γ emitter
	^{24}Na	14.959 hours	^{27}Al(n,α)^{24}Na	γ emitter
	^{23}Na	-	^{27}Al(n,nα)^{23}Na	stable
alpha	^{30}P	4.298 minutes	^{27}Al(a,n)^{30}P	β^+ emitter
	^{30}Si	-	^{27}Al(a,p)^{30}Si	stable
	^{29}P	4.142 seconds	^{27}Al(a,2n)^{29}P	β^+ emitter
	^{29}Al	6.567 minutes	^{27}Al(a,2p)^{29}Al	β^- emitter
proton	^{27}Si	4.16 seconds	^{27}Al(p,n)^{27}Si	β^+ emitter
	^{26}Si	2.234 seconds	^{27}Al(p,2n)^{26}Si	β^+ emitter
deuteron	^{28}Al	2.241 minutes	^{27}Al(d,p)^{28}Al	β^- emitter
	^{27}Mg	9.458 minutes	^{27}Al(d,2p)^{27}Mg	γ emitter
	^{28}Si	-	^{27}Al(d,n)^{28}Si	stable
	^{27}Si	4.160 seconds	^{27}Al(d,2n)^{27}Si	β^+ emitter
	^{25}Mg	-	^{27}Al(d,a)^{25}Mg	stable

Experimentally Identified Residual Radioisotopes

Following neutron exposure of the Al capsule in the G.A. Siwabessy nuclear reactor, there are three pronounced peaks captured by the gamma ray spectroscopy system, at gamma energies of 0.511, 0.844 and 1.368 MeV as can be seen in Fig. 5. The gamma energies of 0.844 MeV and 1.368 MeV clearly correspond to ^{27}Mg and ^{24}Na radioisotopes, respectively. Radioisotope ^{27}Mg identified here, could be due to

^{27}Al(n,p)^{27}Mg and ^{27}Al(d,2p)^{27}Mg nuclear reactions, whereas ^{24}Na is presumably as a result of ^{27}Al(n,α)^{24}Na nuclear reaction. On the other hand, the strong annihilation peak at 0.511 MeV could be due to β^+ emitting radioisotopes such as ^{26}Al from ^{27}Al(n,2n)^{26}Al reaction, and ^{22}Na from ^{27}Al(n,2nα)^{22}Na reaction. Since the observation was conducted 4 days after the Al irradiation in the nuclear reactor, it rules out any involvement of the other short-lived radioisotopes predicted in Table 1 to the strong 0.511 MeV annihilation peak.

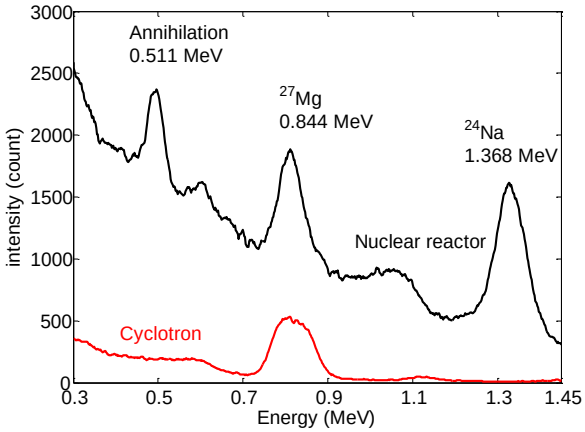

Figure 5 Experimentally observed radioisotopes following Al exposures in the G.A. Siwabessy nuclear reactor and the Radioisotope Delivery System (RDS) 111 Cyclotron

The observed ^{26}Al and ^{22}Na radioisotopes agree with the theoretical calculations previously predicted by Saran and co-workers (Saran *et al* 2012). Moreover, for the first time, our experimental investigation has detected ^{27}Mg radioisotope which has not been reported elsewhere. It should also be noted that the presence of the very long lived ^{26}Al residue (half life = 716,600 years) requires special concern regarding radiation worker's safety when ^{99m}Tc is produced using a nuclear reactor.

As shown in Fig. 5, for proton exposure of the Al body in the RDS 111 cyclotron, there is only a pronounced peak at 0.844 MeV observed experimentally. The 0.844 MeV peak belongs to ^{27}Mg radioisotope, which is due to secondary neutron irradiation of the Al holder via ^{27}Al(n,p)^{27}Mg reaction. In other words, secondary neutrons dominate over the generated secondary particles during the proton bombardment of the Al body, whereas the other secondary particles such as protons, alphas and deuterons were insignificantly produced. In terms of radiation worker's safety, ^{99m}Tc production using a proton-accelerating cyclotron is safer than that of using a nuclear reactor since there are no ^{26}Al or other long lived residues generated.

Conclusions

Theoretical and experimental investigation has been performed to analyze possible isotopes produced during primary neutron and proton irradiation of Al bodies used in ^{99m}Tc production. Various radioactive isotopes and some stable isotopes could be produced during the bombardment. Apart from the primary neutron and proton particles responsible for the creation of residual radioisotopes, there are also some other secondary particles such as alphas and deuterons, which could cause further radioactive and stable isotope production. The resulting radioisotopes have half-lives between 4.142 seconds and 716,600 years with emissions of mostly β^+, γ, and β^-. Experimental results indicate that there are four radioisotopes captured in the gamma ray spectroscopy system following irradiation of Al in the G.A. Siwabessy, namely ^{27}Mg, ^{24}Na, ^{26}Al, and ^{22}Na, whereas only ^{27}Mg is detected after irradiation of Al in the RDS 111 cyclotron. The presence of ^{26}Al residue (half-life = 716,600 years) requires special concern regarding radiation worker's safety when ^{99m}Tc is produced using a nuclear reactor.

Acknowledgments

The authors would like to acknowledge the funding source from the Indonesian National Nuclear Energy Agency (BATAN) and The World Academy of Sciences (TWAS) under the Principal Investigator's

Research Grant Number: 15-020 RG/PHYS/AS_I. Technical assistance by Mr. Bisma Barron Patrianesha and Mr. Abidin is also greatly acknowledged.

References

Bakhtiari, M., Sadeghi, M., Bakht, M. and Ghafoori-Fard, H. (2013) Nuclear model calculations of charged-particle-induced reaction cross section data for the production of the radiohalogen $^{34}Cl^{m}$. Phys. Rev. C, 87: 034621-1 – 03421-12.

Conway, O., Lloyd, S. and Grüning, T. (2013) Global Hepatic Uptake of ^{99m}Tc-MAA During VQ Scintigraphy Secondary to Synchronous Superior and Inferior Vena Caval Obstruction: a Demonstration of Trans-Portal Venous Collateral Pathways. Nucl. Med. Mol. Imaging, 47: 291–293.

de Haro-del Moral, F.J., Sánchez-Lajusticia, A., Gómez-Bueno, M., García-Pavía, P., Salas-Antón, C. and Segovia-Cubero, J. (2012) Role of cardiac scintigraphy with ^{99m}Tc-DPD in the differentiation of cardiac amyloidosis subtype. Rev. Esp. Cardiol. (Engl. Ed.), 65: 440–6.

Gates, V.L., Singh, N., Lewandowski, R.J., Spies, S. and Salem, R. (2015) Intraarterial Hepatic SPECT/CT Imaging Using 99mTc-Macroaggregated Albumin in Preparation for Radioembolization. J. Nucl. Med., 56: 1157–62.

Hillier, S.M., Maresca, K.P., Lu, G.L., Merkin, R.D., Marquis, J.C., Zimmerman, C.N., Eckelman, W.C., Joyal, J.L. and Babich, J.W. (2013) Tc-99m-Labeled Small-Molecule Inhibitors of Prostate-Specific Membrane Antigen for Molecular Imaging of Prostate Cancer. J. Nucl. Med., 54: 1369–1376.

Kambali, I. (2014) Calculated Radioactivity Yields of Cu-64 from Proton-Bombarded Ni-64 Targets Using SRIM Codes. Atom Indonesia, 3: 129–134.

Kambali, I., Suryanto, H. and Parwanto. (2016) Radioactive by-products of a self-shielded cyclotron and the liquid target system for F-18 routine production. Australas. Phys. Eng. Sci. Med., 39: 403–412.

Kambali, I. and Suryanto, H. (2016a) Identification and Angular Distribution of Residual Radionuclides Detected on the Wall of BATAN's Cyclotron Cave. Atom Indonesia, 42: 1–8.

Kambali, I. and Suryanto, H. (2016b). Measurement of Seawater Flow-Induced Erosion Rates for Iron Surfaces using Thin Layer Activation Technique. J. Eng. Technol. Sci., 48: 482–594.

Kinomura, A., Takaki, S., Nakano, Y., Hayashi, Y., Horino, Y. and Abiko, K.. (2002) Neutron Activation Analysis of Ultrahigh-Purity Ti – Al Alloys in Comparison with Glow-Discharge Mass Spectrometry. J-STAGE, 43:116–120.

Koning, A.J. and Rochman, D. (2012) Modern Nuclear Data Evaluation with the TALYS Code System. Nucl. Data Sheets, 113: 2927–2934.

Lu, Y., Groth, J.V. and Emmadi, R. (2015) Cardiac Amyloidosis Detected on Tc-99m Bone Scan. Nucl. Med. Mol. Imaging, 49: 78–80.

Pillai, M.R., Dash, A., Knapp, F.F.Jr. (2013) Sustained Availability of ^{99m}Tc: Possible Paths Forward. J Nucl Med, 54: 313–323.

Pinker, K., Bogner, W., Gruber, S., Brader, P., Trattnig, S., Karanikas, G. and Helbich, T.H. (2011) Molecular imaging in breast cancer - Potential future aspects. Breast Care, 6: 110–119.

Saran, P.K., Nandy, M., Sarkar, P.K., and Goyal, S.L. (2012) Production of long-lived 26Al and 24Na from neutron interaction in Al target. Indian J. Pure Appl. Phys., 50: 509–512.

Saptiama, I., Lestari, E., Sarmini, E., Lubis, H., Marlina and Mutalib, A. (2016) Development of ^{99}Mo/^{99m}Tc Generator System for Production of Medical Radionuclide ^{99m}Tc using a Neutron-activated ^{99}Mo and Zirconium Based Material (ZBM) as its Adsorbent. Atom Indonesia, 42: 115–121.

Silov, G., Taşdemir, A., Özdal, A., Erdoğan, Z., Başbuğ, E.M., Arslan, A.E. and Turhal, Ö. (2014) Radionuclide imaging for breast cancer diagnosis and management: Is technetium-99m tetrofosmin uptake related to the grade of malignancy? Hell. J. Nucl. Med., 17: 87–89.

Vallabhajosula, S., Nikolopoulou, A., Babich, J.W., Osborne, J.R., Tagawa, S.T., Lipai, I., Solnes, L., Maresca, K.P., Armor, T., Joyal, J.L., Crummet, R., Stubbs, J.B. and Goldsmith, S.J. (2014) ^{99m}Tc-Labeled Small-Molecule Inhibitors of Prostate-Specific Membrane Antigen: Pharmacokinetics and Biodistribution Studies in Healthy Subjects and Patients with Metastatic Prostate Cancer. J. Nucl. Med., 55: 1791–8.